Int J Adv Manuf Technol (2018) 94:855–865
DOI 10.1007/s00170-017-0918-5

ORIGINAL ARTICLE

A disk tool cutting method for bevel gear manufacture on a five-axis machine

Yi-Pei Shih[1] · **Zi-Heng Sun**[1] · **Fu-Chuan Wu**[1]

Received: 2 May 2017 / Accepted: 3 August 2017 / Published online: 21 August 2017

Abstract Two main popular cutting methods for bevel gear mass production, face milling and face hobbing, both require dedicated tools and machines available from only a few machine tool companies, which makes production more costly. This paper thus proposes a cheaper, more flexible alternative for producing small or medium batches of large bevel gears, a disk tool cutting method using a five-axis machine. In this method, the machine coordinates are derived based on tooth surfaces. The target's topographic points of tooth surface are applied to construct a fitted surface which is then used to further refine the cutter-contact points to improve the precision of the gear produced. At the same time, mathematical models are established for both the tool and the machine. A coordinate transformation matrix is then generated by aligning the coordinate system of the tool's reference point with each of the work gear cutter-contact points. Because different machines employ identical transformation matrices for producing the same workpiece, the machine's five-axis coordinates can be derived using inverse kinematics. These coordinates are the resource to generate the NC machining data that allows NC verification software to perform cutting simulations. The simulation results verify the correctness of the mathematical models.

Keywords Bevel gear · Disk tool cutting method · Five-axis machine · Fitted surface

✉ Yi-Pei Shih
shihyipei@mail.ntust.edu.tw

[1] Department of Mechanical Engineering, National Taiwan University of Science and Technology, No. 43, Sec. 4, Keelung Rd, Taipei 106, Taiwan, Republic of China

1 Introduction

Because the tooth surfaces of spiral bevel and hypoid gears are too complicated for manufacture, they have traditionally been generated on five- or six-axis machines. The most efficient cutting methods for producing these gears are face milling (FM) and face hobbing (FH), both of which require expensive dedicated machines and special cutting tools. Disk tools and five-axis machines, in contrast, are more affordable and more flexible for manufacturing large gears in small or medium batches. Hence, the Heller company, in cooperation with Gleason, recently introduced a new method for cutting bevel gears on its five-axis machines that replaces a dedicated FM or FH cutter head with a disk milling cutter. The company has not, however, revealed its mathematical model because of commercial considerations. This paper thus proposes a cutting method that reduces current costliness by replacing the multiple heads required for different size gears with one disk tool, making gear manufacture cheaper, more flexible, and able to produce a larger range of gear sizes. This tool can be either a cutter or a wheel for milling or grinding, respectively.

The main mathematical models of FM bevel gears, derived based on a cradle-type bevel gear cutting machine, were established by Litvin and Gutman [1–3], after which Fong [4] proposed a universal mathematical model for simulating all primary bevel gear cutting methods, including FM and FH. These models provide the equations for determining bevel gear tooth surfaces. More recently, Álvarez et al. [5] introduced a flexible cutting method for large-sized spiral bevel gears using a general five-axis machine; however, this method adopted a ball milling cutter that resulted in low productivity. Hence, Shih and Zhang [6] and Shih et al. [7], in establishing both their mathematical model of bevel gear manufacture on a five-axis machine and their flank correction method to reduce manufacturing errors, employed a face milling cutter as the

special cutting tool. In previous work, Deng et al. [8] had developed a mathematical model for producing bevel gears using a disk cutter on a five-axis machine but only provided the cutter's tilt and yaw angles, not the five-axis coordinates for gear production. Chiu and Shih [9] thus proposed a disk tool cutting method for bevel gears on a trunnion-table type five-axis machine with the five-axis coordinates derived virtually based on a cradle-type machine. The tooth surfaces produced by this method, however, still deviated slightly from the theoretical ones because different tools were used.

The disk tool cutting method proposed here is for a five-axis machine whose five-axis coordinates for gear production are derived based on the target tooth surface. First, based on this surface's given topographic points, a B-spline fitted surface is constructed that can then be used to refine the cutter-contact (CC) points on the tooth surface to improve the precision of the gear produced. Mathematical models are also established for both the disk tool and five-axis machine. Next, based on the tool's reference points and the work gear's CC points, all the five-axis coordinates for gear production are derived through inverse kinematics. These coordinates are then used to generate the NC codes that allow the NC verification software to perform simulations and error checks. The results of the cutting simulation verify the correctness of the mathematical models.

2 Construction of fitted surface

Because bevel gear tooth geometries are complicated and depend on cutting method, they are derived from the mathematical models given in references [1–4]. The nominal data for the bevel gears include the gear blank parameters and the position and normal of the topographic points, which are employed for further gear manufacturing or measurement. These specifications can either be calculated from the mathematical models or taken directly from commercial bevel gear design software. To refine the tooth surface CC points for better gear precision, the fitted surface is constructed based on the given topographic points (see Fig. 1) using the B-spline surface fitting technique detailed in reference [10].

The position $\mathbf{r}_1(u, w)$ of the fitted tooth surface is a function of parameters u and w dependent on the defining polygon net (control points $\mathbf{B}_{i,j}$) expressed by Eq. (1). First, however, the fitting parameters must be given, including the degrees of the polynomials in the u−direction and w−direction (k, l) and the numbers of the polygon net edges $n \times m$:

$$\mathbf{r}_1(u,w) = \sum_{i=1}^{n+1}\sum_{j=1}^{m+1} N_{i,k}(u) M_{j,l}(w) \mathbf{B}_{i,j}, \tag{1}$$

where $N_{i,k}$ and $M_{j,l}$ are B-spline basis functions of degrees k and l with respect to parameters u and w. The control points

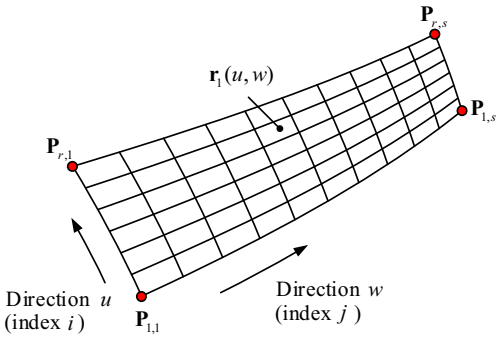

Fig. 1 B-spline surface fitting

are determined from the known surface data (topographic) points [D], which are then interpolated to produce the basis functions whose products [C] are constructed into a matrix: $C_{i,j} = N_{i,k} M_{j,l}$. If [$C$] is not square, the number of control points is smaller than the number of data points, so the control point position vectors [B] can be solved using the least squares method:

$$[B] = \left([C]^T[C]\right)^{-1}[C]^T[D]. \tag{2}$$

Figure 2 shows the fitting tooth surface with one of CC points M, position $\mathbf{r}_1$ and the three orthogonal unit vectors $\boldsymbol{\tau}_1$, $\mathbf{t}_1$, and $\mathbf{n}_1$ of the axes, with $\mathbf{n}_1$ being the surface normal vector obtained from the cross product of the surface's two tangent vectors. Determination of these three axes vectors, which define coordinate system S_{rg}, enables derivation of the machining coordinates.

According to the differential geometry, vectors $\mathbf{Q}_1$ and $\mathbf{T}_1$, which are tangent to the surface at a given point, can be evaluated by differentiating $\mathbf{r}_1$ with respect to parameters u and w as follows:

$$\begin{cases} \mathbf{Q}_1(u,w) = \dfrac{\partial \mathbf{r}_1(u,w)}{\partial u} = \sum\limits_{i=1}^{n+1}\sum\limits_{j=1}^{m+1} N'_{i,k}(u) M_{j,l}(w) \mathbf{B}_{i,j} \\ \mathbf{T}_1(u,w) = \dfrac{\partial \mathbf{r}_1(u,w)}{\partial w} = \sum\limits_{i=1}^{n+1}\sum\limits_{j=1}^{m+1} N_{i,k}(u) M'_{j,l}(w) \mathbf{B}_{i,j} \end{cases}. \tag{3}$$

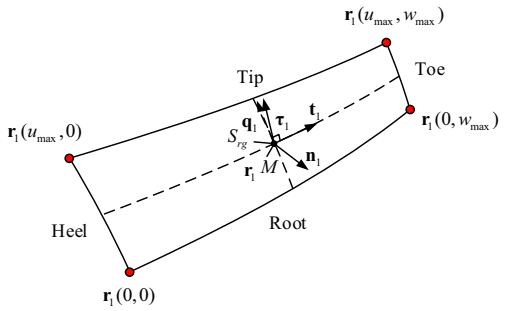

Fig. 2 Fitting tooth surface

The three orthogonal vectors ($\boldsymbol{\tau}_1, \mathbf{t}_1, \mathbf{n}_1$) of the axes are then given by

$$\begin{cases} \mathbf{q}_1(u,w) = \dfrac{\mathbf{Q}_1(u,w)}{|\mathbf{Q}_1(u,w)|}, \mathbf{t}_1(u,w) = \dfrac{\mathbf{T}_1(u,w)}{|\mathbf{T}_1(u,w)|} = \begin{bmatrix} t_{1x} & t_{1y} & t_{1z} \end{bmatrix}^T \\ \mathbf{n}_1(u,w) = \dfrac{\mathbf{t}_1(u,w) \times \mathbf{q}_1(u,w)}{|\mathbf{t}_1(u,w) \times \mathbf{q}_1(u,w)|} = \begin{bmatrix} n_{1x} & n_{1y} & n_{1z} \end{bmatrix}^T \\ \boldsymbol{\tau}_1(u,w) = \mathbf{n}_1(u,w) \times \mathbf{t}_1(u,w) = \begin{bmatrix} \tau_{1x} & \tau_{1y} & \tau_{1z} \end{bmatrix}^T \end{cases}. \tag{4}$$

3 Mathematical model of the disk tool

The tool used here (see Fig. 3) is a milling cutter with inner (IB) and outer (OB) blades, whose coordinate systems S_l and S_t are rigidly connected to both the cutting blade and the tool. Parameters r_0 and $\beta$are the tool's reference radius and rotation angle, whileα_b, α_v, w_p, h_t, and u denote the blade's profile angle, reference angle, point width, reference height, and profile parameter, respectively.

The cutting blade consists of a straight-lined edge and a fillet radius, represented as the following vector equations:

$$\mathbf{r}_l(u) = \begin{bmatrix} x_l(u) & 0 & z_l(u) & 1 \end{bmatrix}^T. \tag{5}$$

The coordinates x_l and z_l of the straight-lined edge and fillet radius, respectively, are

$$\begin{cases} x_l(u) = -u\cos\alpha_b \\ z_l(u) = \mp\left(\dfrac{w_p}{2} + u\sin\alpha_b\right) \end{cases} \quad \text{and} \quad \begin{cases} x_l^{(f)}(u) = -\rho_b + \rho_b\cos u \\ z_l^{(f)}(u) = \mp\left(\dfrac{w_p}{2} - \rho_b\tan(\pi/4 - \alpha_b/2) + \rho_b\sin u\right) \end{cases}.$$

where symbol $\mp$ indicates the inner and outer blade edges. In transition from coordinate system S_l to S_t, the tool position is

$$\mathbf{r}_t(u,\beta) = \mathbf{M}_{tl}(\beta)\mathbf{r}_l(u) = \begin{bmatrix} x_t & y_t & z_t & 1 \end{bmatrix}^T. \tag{6}$$

The corresponding coordinate transformation matrix is

$$\mathbf{M}_{tl}(\beta) = \begin{bmatrix} \cos\beta & \sin\beta & 0 & 0 \\ -\sin\beta & \cos\beta & 0 & 0 \\ 0 & 0 & 1 & 0 \\ 0 & 0 & 0 & 1 \end{bmatrix} \begin{bmatrix} 1 & 0 & 0 & r_0 \\ 0 & 1 & 0 & 0 \\ 0 & 0 & 1 & \rho_b - \rho_b\sin\alpha_v + c_z\cos\alpha_v \\ 0 & 0 & 0 & 1 \end{bmatrix} \begin{bmatrix} \cos\alpha_v & 0 & \sin\alpha_v & 0 \\ 0 & 1 & 0 & 0 \\ -\sin\alpha_v & 0 & \cos\alpha_v & 0 \\ 0 & 0 & 0 & 1 \end{bmatrix},$$

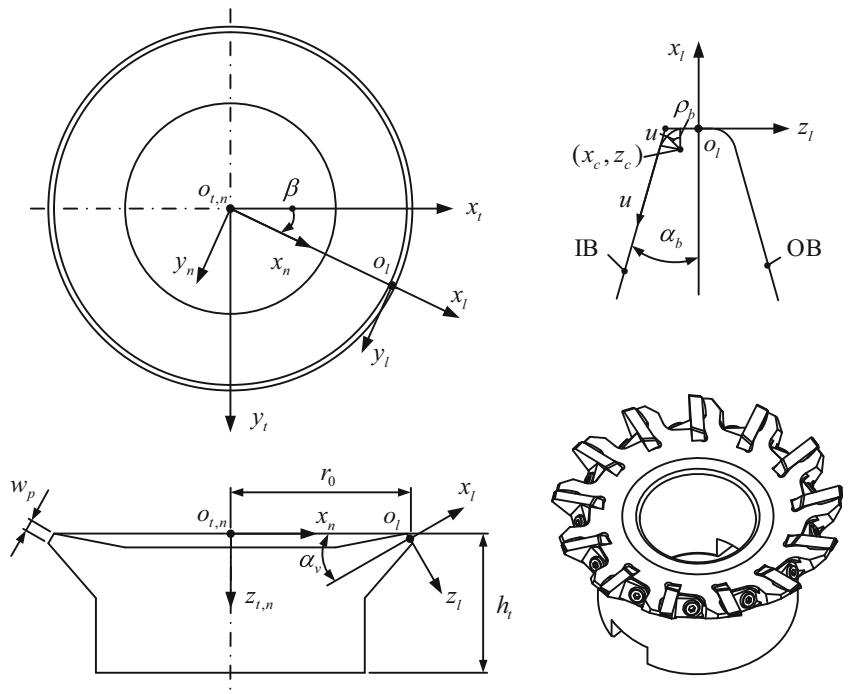

Fig. 3 Coordinate systems for the disk tool

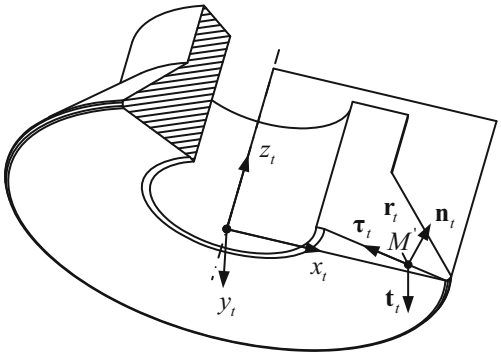

Fig. 4 Disk cutting tool reference point

where

$$c_z = \frac{w_p}{2} - \rho_b \cot\left(\frac{\alpha_b + \pi/2}{2}\right).$$

As Fig. 4 shows, point M on the tool is selected as the reference cutting point, with $\mathbf{n}_t$ as the surface normal vector. The three orthogonal unit vectors ($\boldsymbol{\tau}_t$, $\mathbf{t}_t$, $\mathbf{n}_t$) of the axes, which define coordinate system S_{rt}, are expressed as Eq. (7), which enables derivation of the cutting coordinates.

$$\begin{cases} \boldsymbol{\tau}_t(u,\beta) = \dfrac{\partial \mathbf{r}_t(u,\beta)}{\partial u} \Big/ \left|\dfrac{\partial \mathbf{r}_t(u,\beta)}{\partial u}\right| = [\,\tau_{tx} \quad \tau_{ty} \quad \tau_{tz}\,]^T \\ \mathbf{t}_t(u,\beta) = \dfrac{\partial \mathbf{r}_t(u,\beta)}{\partial \beta} \Big/ \left|\dfrac{\partial \mathbf{r}_t(u,\beta)}{\partial \beta}\right| = [\,t_{tx} \quad t_{ty} \quad t_{tz}\,]^T \\ \mathbf{n}_t(u,\beta) = \mathbf{t}_t(u,\beta) \times \boldsymbol{\tau}_t(u,\beta) = [\,n_{tx} \quad n_{ty} \quad n_{tz}\,]^T \end{cases} \quad (7)$$

4 Coordinate systems of the five-axis machine

Because a five-axis machine has enough degrees of freedom to manufacture complicated bevel gear tooth surfaces, it is flexible enough to replace a dedicated machine, thereby lowering cost. At present, industry employs three main types of five-axis machine: rotary table with tilting head, trunnion table, and double pivot spindle head. The first two have a workpiece rotation axis and so are highly suitable for producing cylinders or cones with features around the periphery, including gears. The tilt head rotary table is particularly suited to manufacturing large gears and is thus adopted here as a numerical example. One such machine, from the Gleason Heller CP series, is illustrated in Fig. 5, which shows its three orthogonally arranged linear axes. The workpiece is positioned on the rotary table and travels along the X axis while the tilting spindle head rotates on the A axis and travels along the $Y$and Z axes. Because the workpiece table is positioned horizontally, the machine is especially suitable for manufacturing heavier parts.

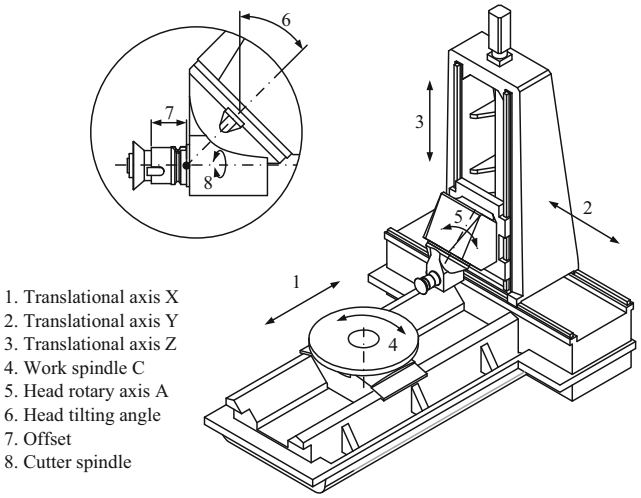

Fig. 5 Configuration of the tilt head rotary table five-axis machine (Gleason Heller CP series)

Before the workpiece can be cut, the program zero for gear production must be defined, as illustrated in Fig. 6 by a right side view of the machine. This reference origin is derived by first aligning the tool axis with the workpiece axis so that the tool can move along the z-axis until its reference point a touches workpiece point b. The coordinates for this location are then recorded as the program zero. The other parameters are M_d, the mounting distance of the work gear; H_f and h_t, the height of the fixture and tool, respectively; and k_z, the offset between pivot point Q and the reference point of tool arbor c.

The coordinate systems of the example machine are shown in Fig. 7, in which the coordinate systems S_t and S_1 are rigidly

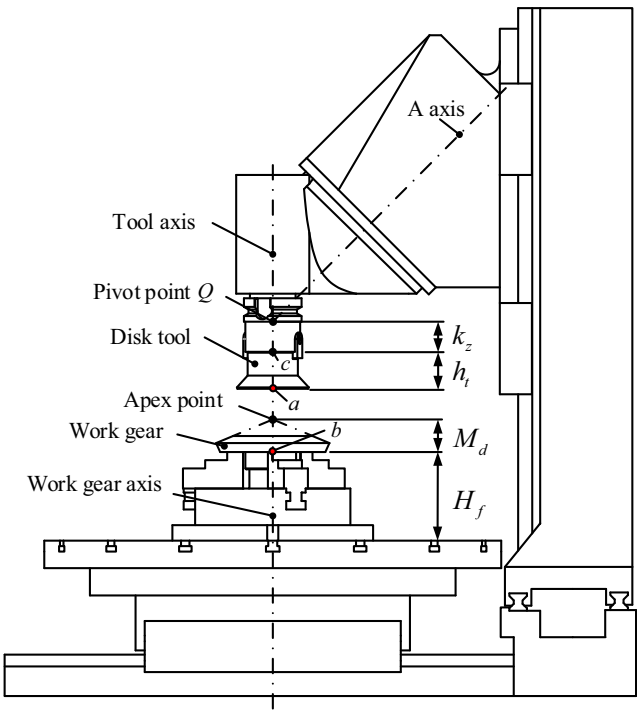

Fig. 6 Program zero for gear production

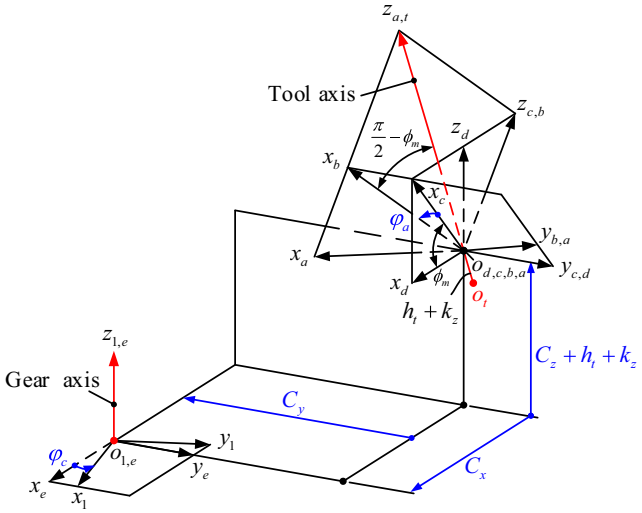

Fig. 7 Coordinate systems for the tilt head rotary table five-axis machine

connected to the disk tool and work gear, respectively, which themselves are positioned by the auxiliary coordinate systems S_a to S_e. Here, C_x, C_y, and C_z are three coordinates for the translational axes, φ_a and φ_c are two coordinates for the rotational axes, and ϕ_m is the tilt angle for the head that, when it equals 45°, enables the tool tilting around the $z_{c,b}$ axis, which

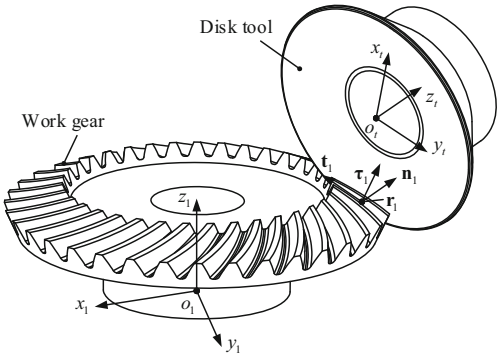

Fig. 8 Relative positions of the disk tool and work gear

is on the $x-z$ plane at a 45° angle to the Z axis. Not shown in the figure is φ_b, the rotation angle of the tool.

The transitional coordinate transformation matrix from coordinate systems S_t and S_1 is represented by

$$\mathbf{M}_{1t}(\varphi_a, \varphi_b, \varphi_c, C_x, C_y, C_z) = \mathbf{M}_{1e}(\varphi_c)\mathbf{M}_{ed}(C_x, C_y, C_z)\mathbf{M}_{dt}(\varphi_a, \varphi_b), \quad (8)$$

with each matrix of the right-hand side of the equation as follows:

$$\mathbf{M}_{dt}(\varphi_a, \varphi_b) = \begin{bmatrix} \cos\varphi_b & \sin\varphi_b & 0 & 0 \\ -\sin\varphi_b & \cos\varphi_b & 0 & 0 \\ 0 & 0 & 1 & -(h_t + k_z) \\ 0 & 0 & 0 & 1 \end{bmatrix} \begin{bmatrix} \cos\phi_m & 0 & \sin\phi_m & 0 \\ 0 & 1 & 0 & 0 \\ -\sin\phi_m & 0 & \cos\phi_m & 0 \\ 0 & 0 & 0 & 1 \end{bmatrix},$$

$$\begin{bmatrix} \cos\varphi_a & \sin\varphi_a & 0 & 0 \\ -\sin\varphi_a & \cos\varphi_a & 0 & 0 \\ 0 & 0 & 1 & 0 \\ 0 & 0 & 0 & 1 \end{bmatrix} \begin{bmatrix} \cos\phi_m & 0 & -\sin\phi_m & 0 \\ 0 & 1 & 0 & 0 \\ \sin\phi_m & 0 & \cos\phi_m & 0 \\ 0 & 0 & 0 & 1 \end{bmatrix}$$

$$\mathbf{M}_{ed}(C_x, C_y, C_z) = \begin{bmatrix} 1 & 0 & 0 & -C_x \\ 0 & 1 & 0 & C_y \\ 0 & 0 & 1 & C_z + h_t + k_z \\ 0 & 0 & 0 & 1 \end{bmatrix}, \text{ and } \mathbf{M}_{1e}(\varphi_c) = \begin{bmatrix} \cos\varphi_c & \sin\varphi_c & 0 & 0 \\ -\sin\varphi_c & \cos\varphi_c & 0 & 0 \\ 0 & 0 & 1 & 0 \\ 0 & 0 & 0 & 1 \end{bmatrix}$$

5 Derivation of the five-axis coordinates for bevel gear tooth surface production

The five-axis machine coordinates for cutting a gear are derived based on the CC points on the target tooth surface. Figure 8 shows the relative position of the disk tool and work gear during the cutting process, with the former tangent to the work gear tooth surface at point M. Aligning the position vector $\mathbf{r}_t$ and three unit vectors ($\mathbf{r}_t(x_t, y_t, z_t)$, $\mathbf{t}_t$, $\boldsymbol{\tau}_t$, $\mathbf{n}_t$) of the axes of the disk tool reference point with those ($\mathbf{r}_1(x_1, y_1, z_1)$, $\mathbf{t}_1$, $\boldsymbol{\tau}_1$, $\mathbf{n}_1$)of the tooth surface CC point yields the transitional transformation matrix from coordinate systems S_{rt} and S_{rg}(Eq. (9)). To produce the same work gear using the same tool, the relative position between the tool and work gear should be as shown in Fig. 8 no matter which machine is used, meaning that the five-axis machine's coordinate transformation matrix $\mathbf{M}_{1t}$ and matrix $\mathbf{M}_{1t}^{(U)}$ must be identical (Eq. (9)). Because each element of the matrix $\mathbf{M}_{1t}^{(U)}$ is derived from known axes parameters (($\mathbf{r}_t$, $\mathbf{t}_t$, $\boldsymbol{\tau}_t$, $\mathbf{n}_t$) and ($\mathbf{r}_1$, $\mathbf{t}_1$, $\boldsymbol{\tau}_1$, $\mathbf{n}_1$)), the five

coordinates can be solved using inverse kinematics as shown in Eq. (10). The tool rotation angle φ_b, however, is irrelevant to the translational coordinates in a milling process.

$$\mathbf{M}_{1t}(\varphi_a,\varphi_b,\varphi_c,C_x,C_y,C_z)=\mathbf{M}_{1t}^{(U)}=\begin{bmatrix} t_{1x} & \tau_{1x} & n_{1x} & x_1\\ t_{1y} & \tau_{1y} & n_{1y} & y_1\\ t_{1z} & \tau_{1z} & n_{1z} & z_1\\ 0 & 0 & 0 & 1\end{bmatrix}\begin{bmatrix} t_{tx} & t_{ty} & t_{tz} & 0\\ \tau_{tx} & \tau_{ty} & \tau_{tz} & 0\\ n_{tx} & n_{ty} & n_{tz} & 0\\ 0 & 0 & 0 & 1\end{bmatrix}\begin{bmatrix} 1 & 0 & 0 & -x_t\\ 0 & 1 & 0 & -y_t\\ 0 & 0 & 1 & -z_t\\ 0 & 0 & 0 & 1\end{bmatrix}=\begin{bmatrix} e_{11} & e_{12} & e_{13} & e_{14}\\ e_{21} & e_{22} & e_{23} & e_{24}\\ e_{31} & e_{32} & e_{33} & e_{34}\\ 0 & 0 & 0 & 1\end{bmatrix}, \tag{9}$$

$$\begin{cases}\varphi_a=\cos^{-1}\left(-\csc^2\phi_m\left(\cos^2\phi_m-e_{33}\right)\right)\\ \varphi_b=\tan^{-1}(x,y)-\delta_c=\tan^{-1}(e_{32},-e_{31})-\delta_c\\ \varphi_c=\tan^{-1}(-e_{23},-e_{13})-\delta_c\\ \delta_c=\tan^{-1}\left(\sin\varphi_a,2\cos\phi_m\sin\frac{\varphi_a^2}{4}\right)\end{cases}\quad\text{and}\quad\begin{cases}C_x=-e_{14}\cos\varphi_c+e_{24}\sin\varphi_c+\sin(2\phi_m)\sin\frac{\varphi_a^2}{4}(h_t+k_z)\\ C_y=e_{14}\sin\varphi_c+e_{24}\cos\varphi_c-\sin\varphi_a\sin\phi_m\sin\frac{\varphi_a^2}{4}(h_t+k_z)\\ C_z=e_{34}-2\sin^2\phi_m\sin\frac{\varphi_a^2}{4}(h_t+k_z)\end{cases}. \tag{10}$$

6 Numerical examples and discussion

The numerical example used here is a spiral bevel gear pair generated by the duplex-helical method (SGDH), whose basic parameters and gear blank data are listed in Table 1. The nominal gear data are determined according to references [4, 11, 12]. In the proposed method, the 11 × 7 topographic points of the tooth surface are further fitted based on a B-spline surface with the 11 × 7 control points of the pinion and ring gear calculated from Eq. (2) (see Table 2 for a partial listing). Degrees k and l of B-spline basis functions are four. A refined set of 15 × 7 CC points on the tooth surface is then generated from Eq. (1) to satisfy the demand for manufacturing precision. The orthogonal unit vectors of each point (partially listed in Table 3) are further calculated based on Eqs. (3) and (4). The symbols i and j in the following tables indicate row and column numbers (see Fig. 1).

The parameters of the disk tool and five-axis machine are given in Table 4. As stipulated in reference [8], the cutter radius must be neither too large nor too small to avoid

Table 1 Basic parameters for the example pair

Items		Pinion		Ring gear	
		Convex	Concave	Convex	Concave
(A) Basic gear data					
Number of teeth	z	20		40	
Outer module	m_{et}	6.000			
Pressure angle	α_n	20.000°			
Spiral angle	β_m	35.000° L.H.		35.000° R.H.	
(B) Gear blank data					
Pitch angle	δ	26.565°		63.435°	
Face angle	δ_a	31.274°		65.728°	
Outer diameter	d_{ae}	133.010		243.167	
Outer whole depth	h_e	12.118			
Face width	b	40.000			
Mounting distance	M_d	128.000		76.000	
(C) Assembly data					
Shaft angle	Σ	90.000°			
Offset	V	0.000		–	
Axial setting	H	0.000		0.000	
(D) FM cutter data					
Profile angle	α_b	22.667°	17.333°	22.667°	17.333°
Cutter radius	r_0	133.008	135.608	133.008	135.608
Fillet radius	ρ_b	1.200	1.200	1.200	1.200

Table 2 Control points on the gear's fitted tooth surfaces: pinion and ring gear (partial list)

		Pinion						Ring gear					
		Convex			Concave			Convex			Concave		
j	i	x_1	y_1	z_1	x_1	y_1	z_1	x_1	y_1	z_1	x_1	y_1	z_1
1	1	−39.287	8.516	42.821	−38.259	12.491	42.845	−81.745	−9.650	30.068	−81.216	−13.824	30.212
1	4	−42.318	7.876	44.243	−40.521	14.576	44.252	−83.275	−8.600	32.877	−82.363	−15.212	32.953
1	7	−45.183	6.645	45.556	−42.362	17.063	45.556	−84.770	−7.367	35.623	−83.419	−16.778	35.623
6	1	−48.653	−3.477	24.207	−48.845	1.013	24.301	−99.905	2.551	19.582	−99.987	−2.147	19.852
6	4	−52.434	−5.594	26.181	−52.667	2.918	26.247	−101.776	4.321	23.443	−101.81	−3.808	23.594
6	7	−55.729	−8.532	28.002	−56.067	5.609	28.046	−103.562	6.358	27.215	−103.542	−5.764	27.238
11	1	−53.747	−18.542	6.428	−55.267	−13.941	6.499	−115.302	18.227	9.468	−116.166	13.132	9.813
11	4	−57.639	−22.507	8.936	−60.604	−12.781	8.966	−117.347	20.867	14.373	−118.743	11.271	14.552
11	7	−60.607	−27.381	11.253	−65.678	−10.451	11.253	−119.223	23.842	19.167	−121.250	8.999	19.167

overcutting on the concave or convex side. Figure 9 shows the cutter profiles of the pinion and ring gear disk tools, in which the former must be arranged in the opposite direction to the latter for solving machine coordinates. Tool wear can be reduced by selecting different disk tool reference points for different cutting depths. The position vector and three unit vectors of the cutting tool reference points are calculated from Eqs. (6) and (7) and those for the pinion and ring gear are

Table 3 CC points on the gear's fitted tooth surfaces: position and vectors (partial list)

		Position			Tangential vector, u			Tangential vector, w			Normal vector		
j	i	x_1	y_1	z_1	τ_{1x}	τ_{1y}	τ_{1z}	t_{1x}	t_{1y}	t_{1z}	n_{1x}	n_{1y}	n_{1z}
(a) Convex flank of pinion													
1	1	−39.287	8.516	42.821	−0.852	−0.043	0.522	−0.46	−0.418	−0.784	−0.252	0.908	−0.336
1	7	−45.183	6.645	45.556	−0.687	−0.257	0.679	−0.505	−0.503	−0.701	−0.522	0.825	−0.216
8	4	−52.365	−5.66	26.183	−0.679	−0.378	0.63	−0.316	−0.624	−0.715	−0.663	0.684	−0.305
15	1	−53.747	−18.542	6.428	−0.698	−0.465	0.544	−0.117	−0.676	−0.728	−0.706	0.572	−0.417
15	7	−60.607	−27.381	11.253	−0.433	−0.546	0.717	−0.071	−0.772	−0.631	−0.899	0.324	−0.296
(b) Concave flank of pinion													
1	1	−38.259	12.491	42.845	−0.829	0.47	0.304	−0.503	−0.386	−0.773	0.246	0.794	−0.556
1	7	−42.362	17.063	45.556	−0.667	0.712	0.217	−0.608	−0.353	−0.711	0.43	0.607	−0.669
8	4	−52.607	2.905	26.247	−0.899	0.375	0.226	−0.414	−0.562	−0.716	0.141	0.737	−0.661
15	1	−55.267	−13.941	6.499	−0.954	−0.069	0.291	−0.172	−0.67	−0.722	−0.245	0.739	−0.628
15	7	−65.678	−10.451	11.253	−0.958	0.232	0.171	−0.287	−0.704	−0.649	0.03	0.671	−0.741
(c) Convex flank of ring gear													
1	1	−81.745	−9.65	30.068	−0.367	0.24	0.899	−0.792	0.426	−0.437	0.488	0.872	−0.033
1	7	−84.77	−7.367	35.623	−0.236	0.275	0.932	−0.81	0.475	−0.345	0.537	0.836	−0.11
8	4	−101.745	4.369	23.443	−0.25	0.288	0.924	−0.7	0.605	−0.378	0.669	0.742	−0.05
15	1	−115.302	18.227	9.468	−0.267	0.311	0.912	−0.573	0.71	−0.41	0.775	0.632	0.011
15	7	−119.223	23.842	19.167	−0.132	0.293	0.947	−0.558	0.767	−0.315	0.819	0.57	−0.063
(d) Concave flank of ring gear													
1	1	−81.216	−13.824	30.212	−0.561	−0.31	0.768	−0.809	0.402	−0.429	0.176	0.862	0.476
1	7	−83.419	−16.778	35.623	−0.492	−0.433	0.756	−0.861	0.371	−0.348	0.13	0.822	0.555
8	4	−101.782	−3.782	23.594	−0.589	−0.287	0.755	−0.749	0.545	−0.377	0.303	0.788	0.536
15	1	−116.166	13.132	9.813	−0.636	−0.109	0.764	−0.602	0.689	−0.403	0.483	0.717	0.504
15	7	−121.25	8.999	19.167	−0.619	−0.261	0.741	−0.668	0.67	−0.323	0.412	0.695	0.589

Table 4 Disk tool and five-axis machine parameters

Items		Pinion	Ring gear
(A) Disk tool			
Point width	w_p	1.500	
Profile angle	α_b	19.000°	
Reference angle	α_v	30.000°	
Cutter radius	r_0	50.000	
Fillet radius	ρ_b	0.800	
Reference height	h_t	14.000	27.000
(B) Five-axis machine			
Head tilt angle	ϕ_m	45.000°	
Machine offset	k_z	95.000	75.000

listed in Table 5. Each matrix $\mathbf{M}_{1t}^{(U)}$ can be calculated from the selected disk tool reference point and those $(\mathbf{r}_1, \mathbf{t}_1, \boldsymbol{\tau}_1, \mathbf{n}_1)$ of each work gear CC point. The five-axis coordinates for these latter are then determined according to Eq. (10) and partially listed in Table 6.

The numerical control (NC) codes for cutting are generated based on the five coordinates listed in Table 6, whose positions are tested for errors using the NC verification software VERICUT. The NC codes are also used to perform cutting simulations for the pinion and ring gear (displayed in Fig. 10). After simulation, the finished gears are exported as STL (StereoLithography) files whose left side is shown in Fig. 11. The flank topographic deviations between the STL and theoretic tooth surfaces are then evaluated using a program developed by the authors. Figure 11a, b (right side) show the results for the pinion and ring gear: average error = 0.0 and $0.0\mu m$, sum of the square = 4 , 048and 5 , $457\mu m^2$, and tooth space error = −0.2and $-0.9\mu m$, respectively. These errors, which could result from simulation error (with an interpola-

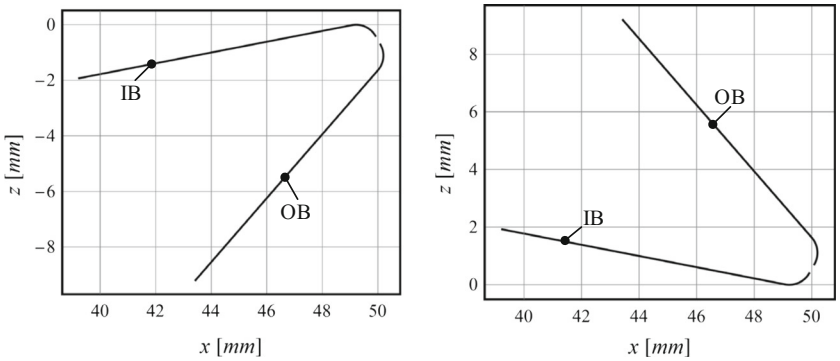

(a) Pinion (b) Ring gear

Fig. 9 Disk tool profiles in gear cutting

Table 5 Disk tool reference points (partial list)

	Parameter		Position, $\mathbf{r}_t$			Tangent, $\boldsymbol{\tau}_t$	Tangent, $\mathbf{t}_t$	Normal $\mathbf{n}_t$
i	u	β	x_t	y_t	z_t			
(a) Inner blade for the convex flank of pinion								
1	1.5	0.0	48.153	0.000	−0.192	(−0.982, 0, −0.191)	(0, −1, 0)	(0.191, 0, −0.982)
4	1.6	0.0	47.858	0.000	−0.249			
7	1.7	0.0	47.564	0.000	−0.307			
(b) Outer blade for the concave flank of pinion								
1	1.8	0.0	49.194	0.000	−2.563	(−0.656, 0, −0.755)	(0, −1, 0)	(0.755, 0, −0.656)
4	1.9	0.0	48.997	0.000	−2.790			
7	2.0	0.0	48.800	0.000	−3.016			
(c) Inner blade for the convex flank of ring gear								
1	1.5	0.0	48.153	0.000	0.192	(−0.982, 0, 0.191)	(0, −1,0)	(−0.191, 0, −0.982)
4	1.6	0.0	47.858	0.000	0.249			
7	1.7	0.0	47.564	0.000	0.307			
(d) Outer blade for the concave flank of ring gear								
1	1.8	0.0	49.194	0.000	2.563	(−0.656, 0, 0.755)	(0, −1, 0)	(−0.755, 0, −0.656)
4	1.9	0.0	48.997	0.000	2.79			
7	2	0.0	48.800	0.000	3.016			

Table 6 Five-axis coordinates for finish cutting the gears (partial list)

		Convex flank					Concave flank				
j	i	φ_a	φ_c	C_x	C_y	C_z	φ_a	φ_c	C_x	C_y	C_z
(a) Pinion											
1	1	133.898	−136.465	78.335	34.832	−44.833	106.625	−92.308	95.816	22.585	−24.993
1	4	123.997	−123.047	86.556	27.654	−42.400	113.207	−101.706	94.466	22.005	−33.597
1	7	112.891	−107.067	96.042	19.025	−39.645	127.979	−119.247	90.548	26.275	−48.342
8	1	140.818	−122.914	84.857	32.988	−33.805	111.436	−77.426	99.939	14.940	−13.337
8	4	129.957	−109.053	92.196	24.377	−30.903	118.311	−87.217	98.911	16.437	−21.667
8	7	117.814	−92.474	100.098	14.435	−27.111	133.340	−105.367	95.413	23.993	−35.675
15	1	146.618	−107.270	91.031	30.549	−20.749	116.736	−62.271	102.711	7.848	−1.058
15	4	135.028	−93.352	97.114	20.525	−17.506	123.098	−71.679	102.222	10.779	−8.381
15	7	122.667	−77.198	102.991	9.898	−13.276	136.769	−88.658	99.960	20.042	−20.545
(b) Ring gear											
1	1	121.048	7.353	199.512	−34.342	−14.569	130.908	−8.640	202.414	−8.040	−20.336
1	4	126.539	2.486	202.234	−22.410	−23.496	126.819	−3.073	200.339	−18.477	−22.984
1	7	132.299	−2.650	204.029	−8.953	−32.673	120.491	4.228	196.065	−33.212	−24.341
8	1	117.726	−1.738	179.371	−33.891	−4.571	128.207	−17.263	182.933	−10.985	−10.885
8	4	123.281	−6.368	182.797	−23.706	−12.637	124.244	−11.932	181.316	−19.566	−12.619
8	7	129.057	−11.246	185.417	−12.118	−20.923	118.416	−5.087	177.973	−31.301	−13.292
15	1	115.326	−11.482	159.108	−34.108	5.234	126.012	−26.450	163.261	−14.918	−1.347
15	4	120.601	−15.673	163.026	−25.930	−1.697	122.572	−21.575	162.26	−21.191	−2.429
15	7	126.254	−20.252	166.407	−16.207	−8.954	117.696	−15.513	160.045	−29.555	−2.730

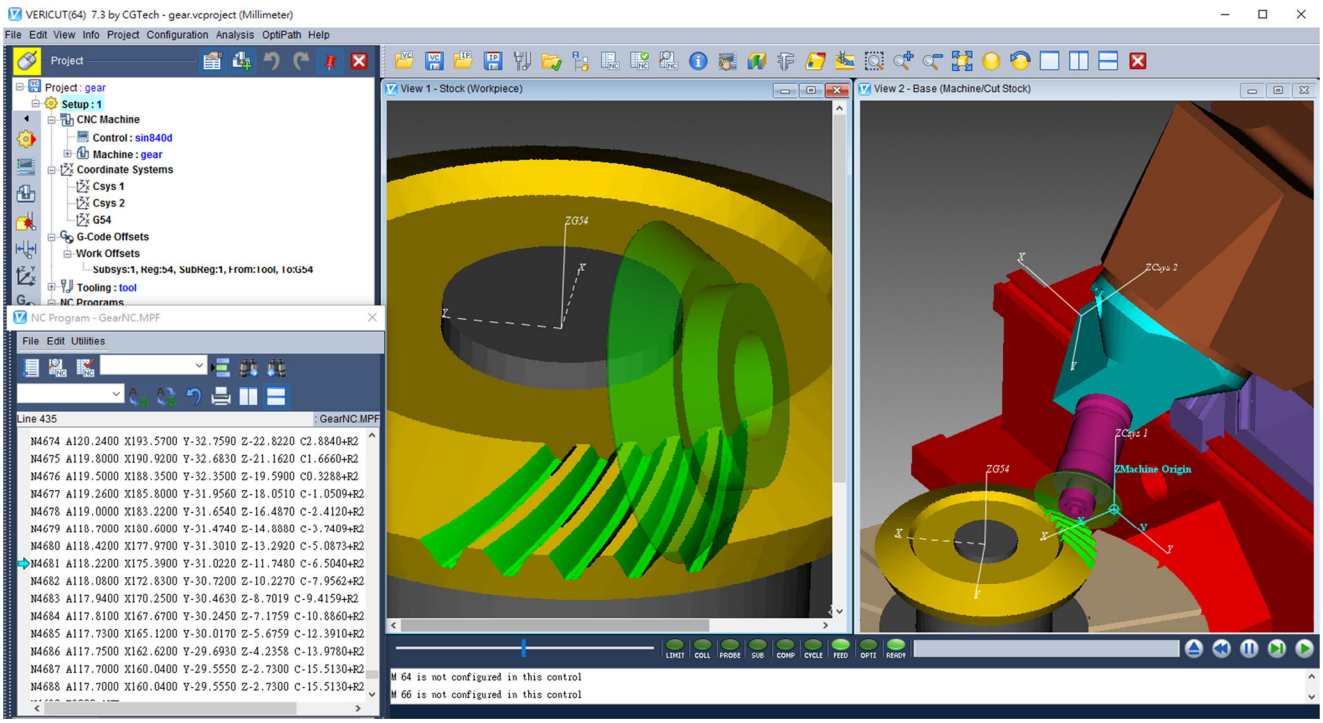

Fig. 10 Cutting simulation for the gear using VERICUT

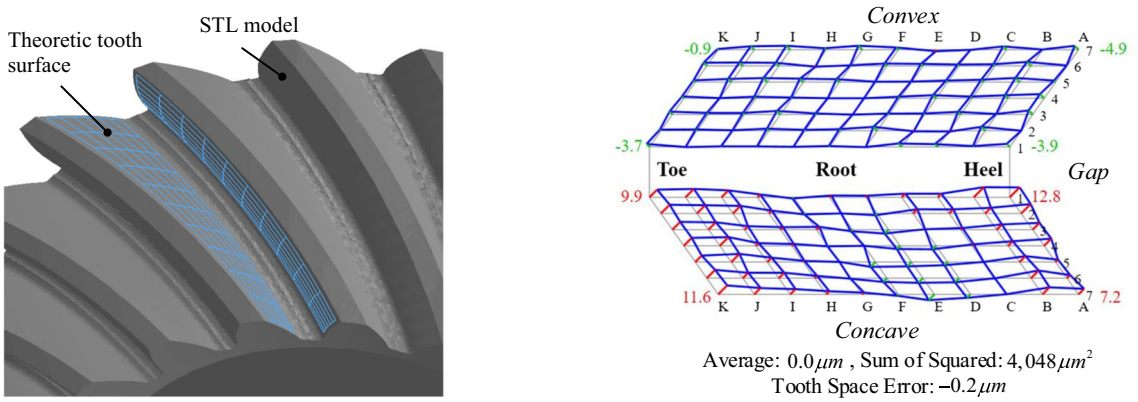

(a) Pinion

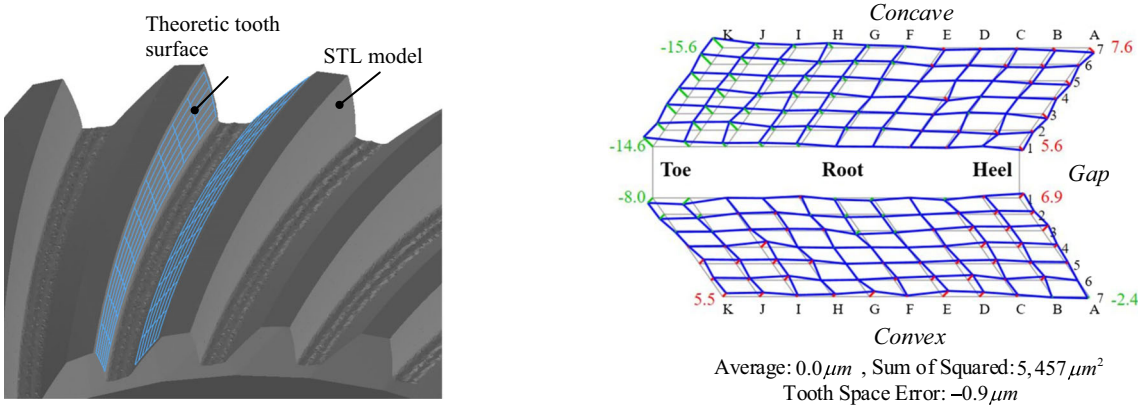

(b) Ring gear

Fig. 11 Topographic deviations of the gear flank produced by VERICUT simulation

tion tolerance of 0.05 mm in VERICUT), are small enough to confirm the correctness of the five-axis coordinates (videos of the cutting simulations for the pinion and gear are available on the web, see [13, 14]).

7 Conclusions

A five-axis machine with a disk tool is a good choice for manufacturing small or medium batches of large bevel gears because it is less costly and more flexible than a dedicated machine. This paper therefore proposes a disk tool cutting method for bevel gears in which the dedicated tool is replaced by a disk tool on a tilt head rotary table five-axis machine. Once the mathematical models for the tool and machine are established, the coordinate transformation matrices for all CC points on the tooth surface are determined by aligning the coordinate system of the disk tool reference point with that of each work gear CC point. No matter the machine type, the coordinate transformation matrices are identical whenever the same tool is used to produce the same workpiece, allowing derivation of the five-axis coordinates for gear production through inverse kinematics. These CC point coordinates are necessary for generating the NC codes, which are used by the NC verification software VERICUT to perform cutting simulations for both pinion and ring gear. This software also generates STL gear files for further evaluation of the extent to which the simulation outcomes deviate from the theoretical ones. According to this error analysis, the deviations are small enough to successfully confirm the correctness of the mathematical models.

α_b, profile angle of the blade; α_v, reference angle of the blade; β, rotation angle of the disk tool; C_x, C_y, C_z, translating coordinates for the five-axis machine; φ_a, φ_c, rotation coordinates for the five-axis machine; φ_b, spindle angle for the five-axis machine; h_t, reference height of the disk tool; k_z, distance between the pivot point Q and the reference point of tool arbor c; $\mathbf{M}_{ij}$, homogeneous transformation matrix from coordinate system S_j to coordinate system S_i; $\mathbf{n}_1$, $\mathbf{t}_1$, $\boldsymbol{\tau}_1$, three orthogonal unit vectors of the work gear CC point; $\mathbf{n}_t$, $\mathbf{t}_t$, $\boldsymbol{\tau}_t$, three orthogonal unit vectors of the disk tool reference point; r_0, cutter radius; $\mathbf{r}_1$, position vector of the work gear's topographic point; $\mathbf{r}_t$, position vector of the disk tool reference point; ρ_b, fillet radius of the blade; u, parameter of the cutting edge; w_p, point width of the blade; $[B]$, matrix of the three-dimensional coordinates of the control points; $[C]$, matrix of the products of the basic functions; $[D]$, matrix of the three-dimensional coordinates of the surface data points.

Acknowledgments The authors are grateful to the R.O.C.'s Ministry of Science and Technology for its financial support. Part of this work was performed under Contract No. MOST 104-2221-E-011-102. The authors also give special thanks to Dr. B.T. Sheen for his technical support in the cutting experiment.

References

1. Litvin FL, Gutman Y (1981) Methods of synthesis and analysis for hypoid gear-drives of "formate" and "helixform"—Part 1. Calculations for machine settings for member gear manufacture of the formate and helixform hypoid gears. ASME J Mech Des 103(1):83–88
2. Litvin FL, Gutman Y (1981) Methods of synthesis and analysis for hypoid gear-drives of "formate" and "helixform"—Part 2. Machine setting calculations for the pinions of formate and helixform gears. ASME J Mech Des 103(1):89–101
3. Litvin FL, Gutman Y (1981) Methods of synthesis and analysis for hypoid gear-drives of "formate" and "helixform"—Part 3. Analysis and optimal synthesis methods for mismatch gearing and its application for hypoid gears of "formate" and "helixform". ASME J Mech Des 103(1):102–110
4. Fong ZH (2000) Mathematical model of universal hypoid generator with supplemental kinematic flank correction motions. ASME J Mech Des 122(1):136–142
5. Álvarez A, López de Lacalle LN, Olaiz A, Rivero A (2015) Large spiral bevel gears on universal 5-axis milling machines: a complete process. Proc Eng 132:397–404
6. Shih YP, Zhang CX (2017) Manufacture of spiral bevel gears using standard profile angle blade cutters on a five axis computer numerical control machine. J Manuf Sci Eng 139(6):061017 (14 pages)
7. Shih YP, Sun ZH, Lai KL (2017) A flank correction face-milling method for bevel gears using a five-axis CNC machine. Int J Adv Manuf Technol. doi:10.1007/s00170-017-0032-8
8. Deng XZ, Li GG, Wei BY, Deng J (2014) Face-milling spiral bevel gear tooth surfaces by application of 5-axis CNC machine tool. Int J Adv Manuf Tech 71(5):1049–1057
9. Chiu CM, Shih YP Spiral bevel gear manufacturing on a CNC five-axis machine using bell-type milling cutters. Proceedings of the 2014 IFToMM Asian MMS, Tianjin, China
10. Rogers DF, Adams JA (1990) Mathematical elements for computer graphics, second edn. McGraw-Hill, New York
11. Works G (1971) Calculation instructions: generated spiral bevel gears, duplex-helical method, including grinding. Gleason Works, Rochester
12. Litvin FL, Fuentes A (2004) Gear geometry and applied theory, second edn. Cambridge University Press, Cambridge
13. Video of the cutting simulations for pinion: https://www.youtube.com/watch?v=b_jVz25eGlk&list=UUEIBxFzAEhFaFOL4w0E07g&index=1
14. Video of the cutting simulations for gear: https://www.youtube.com/watch?v=_FKGfZKhbRU&list=UUEIBxFzAEhFaFOL4w0E07g&index=2